Title
Understanding the role of carbamate reactivity in fatty acid amide hydrolase inhibition by QM/MM mechanistic modelling.

Journal
Chemical communications (Cambridge, England), 47(9)

Authors
Piomelli, D
Lodola, A
Capoferri, L
et al.

Publication Date
2011-03-07

DOI
10.1039/c0cc04937a

ChemComm

Cite this: *Chem. Commun.*, 2011, **47**, 2517–2519

www.rsc.org/chemcomm

COMMUNICATION

Understanding the role of carbamate reactivity in fatty acid amide hydrolase inhibition by QM/MM mechanistic modellingw

Alessio Lodola,*[a] Luigi Capoferri,[a] Silvia Rivara,[a] Ewa Chudyk,[b] Jitnapa Sirirak,[b] Edyta Dyguda-Kazimierowicz,[c] W. Andrzej Sokalski,[c] Mauro Mileni,[d] Giorgio Tarzia,[e] Daniele Piomelli,[f] Marco Mor[a] and Adrian J. Mulholland*[b]

Received 12th November 2010, Accepted 21st December 2010
DOI: 10.1039/c0cc04937a

QM/MM modelling of FAAH inactivation by ***O***-biphenyl-3-yl carbamates identifies the deprotonation of Ser241 as the key reaction step, explaining why FAAH is insensitive to the electron-donor e ect of conjugated substituents; this may aid design of new inhibitors with improved selectivity and ***in vivo*** potency.

Carbamate-based compounds are widely used as covalent inhibitors of serine hydrolases of therapeutic interest, including fatty acid amide hydrolase (FAAH).[1] This enzyme is characterized by an uncommon Ser-Ser-Lys catalytic triad. It is the main enzyme responsible for the hydrolysis of the endocannabinoid anandamide. Despite its unusual catalytic mechanism,[2–4] FAAH is inhibited by classical serine hydrolase inhibitors,[1] and by O-biphenyl-3-yl carbamates, which are promising clinical candidates for the treatment of central nervous system and peripheral disorders.[5]

These carbamate inhibitors, e.g. URB524 (Fig. 1), can be docked in two possible orientations (called orientations I and II) within the FAAH catalytic site.[6,7] Recently, hybrid quantum mechanical/molecular mechanics (QM/MM) modelling,[8] using the B3LYP/6-31G(d)//PM3-CHARMM22 potential, showed that the inhibitory process is energetically preferred in orientation II.[9] This orientation allows the catalytic nucleophile, Ser241, to e ciently attack the carbonyl group of URB524 (Fig. 2), yielding a carbamoylated enzyme.[10]

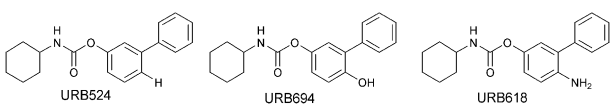

Fig. 1 FAAH inhibitors employed in the present investigation.

[a] Dipartimento Farmaceutico, Università degli Studi di Parma, 43124 Parma, Italy. E-mail: Alessio.Lodola@unipr.it
[b] School of Chemistry, University of Bristol, Bristol, BS8 1TS, UK. E-mail: Adrian.Mulholland@bristol.ac.uk
[c] Department of Chemistry, Wrocław University of Technology, Wyb. Wyspianskiego 27, Wrocław, Poland
[d] Department of Molecular Biology, The Scripps Research Institute, La Jolla, CA 92037, USA
[e] Dipartimento di Scienze del Farmaco e della Salute, Università degli Studi di Urbino ''Carlo Bo'', 61029 Urbino, Italy
[f] Department of Drug Discovery and Development, Italian Institute of Technology, 16163, Genova, Italy
w Electronic supplementary information (ESI) available: Details of QM/MM and DTSS calculations. See DOI: 10.1039/c0cc04937a

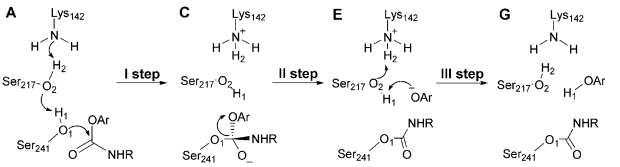

Fig. 2 Steps of Ser241 carbamoylation in FAAH by biphenyl-3-yl carbamates. A, C, E, G are significant intermediates along the reaction pathway. Labels refer to the reaction coordinates defined in the text.

This prediction has been recently confirmed by the crystallographic structure of the FAAH-URB597 carbamoylated adduct,[11] showing the reliability of this QM/MM approach for FAAH.

In vitro potency of FAAH inhibitors depends on a combination of covalent binding to the catalytic Ser241 and noncovalent interactions with specific recognition elements in the active site of FAAH,[7] while in vivo potency is also a ected by plasmatic stability.[12] Structure–activity relationship (SAR) studies showed that conjugated, electron-donor groups on the biphenyl sca old of URB524 (which increase electron density around the carbamate carbon) are associated with enhanced carbamate stability both in alkaline bu er and in rat plasma.[13] Conversely, these groups do not a ect FAAH inhibitor potency in vitro.[7] To understand this apparent discrepancy, we here apply a QM/MM approach to model the carbamoylation reaction of FAAH by the reference inhibitor URB524 (IC_{50} = 25.6 nM) and by its p-OH (URB694, IC_{50} = 30.0 nM) and p-NH_2 (URB618, IC_{50} = 27.2 nM) derivatives (Fig. 1). Furthermore, di erential transition state stabilization (DTSS) analysis,[14] an emerging approach for identifying important interactions in enzyme-catalysed reactions,[15] was also performed to identify crucial residues involved in FAAH inhibition.

The QM/MM calculations show that carbamoylation of Ser241 takes place with a similar mechanism, and similar energetic barriers, for the three inhibitors, with formation of the tetrahedral intermediate (TI) being the rate-limiting step of the inhibitory process. Electron donor substituents do not significantly a ect the key transition state (TS) of the reaction, in agreement with experimental findings. This provides an explanation of the activity of URB524 analogues, as discussed below.

Michaelis complexes of FAAH with carbamate inhibitors were built according to the energetically preferred[9] and

experimentally observed[11] binding orientation II.[16] The resulting structures were solvated by a 25 Å-radius sphere of TIPS3P water molecules and equilibrated by 250 ps of molecular dynamics.[9] The equilibrated complexes were employed for QM/MM reaction modelling at the PM3-CHARMM22 level [details in the ESIw], with DFT energy corrections.[17]

A coordinate driving approach[18] was used to explore potential energy surfaces (PESs) for Ser241 carbamoylation. The reaction was modelled in three steps (Fig. 2) starting from the Michaelis complex (A): (1) formation of the TI (C); (2) m-biphenate expulsion with formation of carbamoylated Ser241 (E); (3) m-biphenate protonation and formation of neutral Lys142 (G). Other mechanisms were also tested (e.g. TI protonation followed by biphenyl-3-ol expulsion) but as found previously for URB524,[9] only the mechanism reported here was found to be energetically and structurally reasonable.

Formation of the TI was modelled by restraining two reaction coordinates: Rx = [d(O_1, H_1) − d(O_2, H_1) − d(O_1, C)] describing proton abstraction from Ser241 by Ser217 and nucleophilic attack by Ser241; Ry = [d(O_2, H_2) − d(N_1, H_2)] describing the proton transfer between Ser217 and Lys142. m-Biphenate expulsion was modelled by breaking the C–O bond, restraining Rz = [d(C, O_{Ar})]. The third step, including the final proton transfers, was based on Rr = [d(O_2, H_1) − d(O_{Ar}, H_1)], to move proton H_1 from Ser217 to the m-biphenate oxygen, and Rs = [d(N_1, H_2) − d(O_2, H_2)], to transfer H_2 from Lys142 to Ser217. Rx, Ry, Rz, Rr, and Rs were increased in steps of 0.1 Å, applying harmonic restraints of 5000 kcal mol^{-1} Å^{-2}. For each value of the reaction coordinates, the energy was computed by single point calculation at the PM3-CHARMM22 level, removing the energy contribution due to reaction coordinate restraints. Higher level calculations (B3LYP/6-31 + G(d))[17] were used to correct the energies of crucial stationary points (intermediates and approximate TS structures) from the PM3-CHARMM22 PESs, similarly to refs. 3, 9 and 19.

The optimized structures of the reactants (Michaelis complexes) indicate that the three inhibitors bind similarly in the FAAH active site, with the O-biphenyl moiety within the cytoplasmic access (CA) channel and the N-cyclohexyl group occupying the acyl-chain-binding (ACB) pocket of FAAH. The inhibitor carbonyl oxygen is placed in the oxyanion hole, undertaking one hydrogen bond with Ile238, and three weaker polar interactions with backbone NHs of Gly239, Gly240 and Ser241. The hydroxyl of Ser241 is close to the carbamate carbon, and forms a hydrogen bond network with Ser217 and Lys142. For URB694 (Fig. 3) and URB618, the substituent in the para position forms a hydrogen bond with the backbone NHs of Cys269 and Val270 via a water molecule (here named Wat627), conserved in crystallographic structures.[20]

Fig. 4 shows the resulting B3LYP/6-31 + G(d)//PM3-CHARMM22 energy profiles for carbamoylation of Ser241 by URB524 (blue), URB694 (red) and URB618 (green), starting from the corresponding Michaelis complexes (A). The reaction starts with a double proton transfer, in which Lys142, in cooperation with the bridging Ser217,[3] deprotonates Ser241, triggering the nucleophilic attack and formation of the TI (C).

Consistent with our previous findings,[9] formation of the TI, rather than its protonation and collapse, is the rate limiting

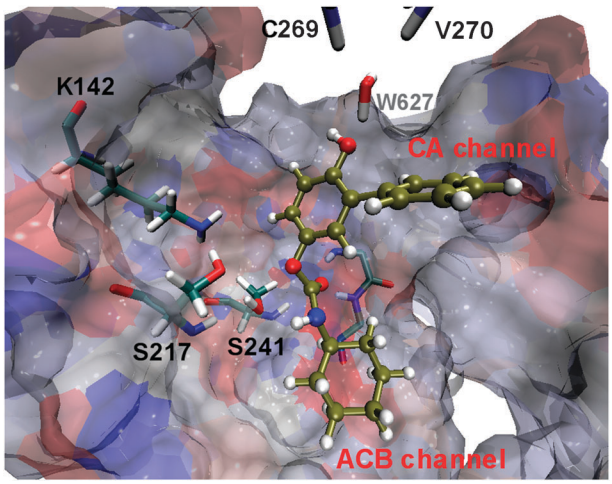

Fig. 3 FAAH–URB694 Michaelis complex. Carbon atoms of FAAH are coloured in cyan, and those of URB694 in brown. The van der Waals surface of FAAH is coloured according to amino acid formal charge.

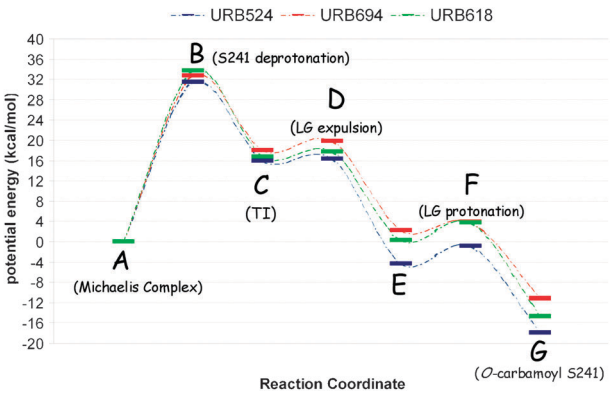

Fig. 4 B3LYP/6-31 + G(d)//PM3-CHARMM22 energy profiles for carbamoylation of Ser241 by carbamate inhibitors.

step (largest barrier) for FAAH inactivation. The B3LYP/6-31 + G(d)//PM3-CHARMM22 barriers for this crucial step are similar for the three inhibitors (31.5 kcal mol^{-1} for URB524, 32.7 kcal mol^{-1} for URB694 and 33.6 kcal mol^{-1} for URB618), despite their di erent chemical structure and reactivity. Thus, introduction of conjugated, electron-donor groups (OH, σ_p = −0.37 and NH_2, σ_p = −0.66)[21] does not significantly a ect the overall shape of the energy profiles, nor the energy of the important TS of the reaction in FAAH. This indicates that the electronic distribution of the carbamate has a negligible e ect on Ser241 carbamoylation, in spite of its profound importance for chemical and plasmatic stability of these compounds.[12] This can be understood as this TS structure is characterized by deprotonation of Ser241 (H_1 is found between O_1 and O_2), with the nucleophile O_1 still approaching the carbonyl carbon of the inhibitor (Table 1).

The TI (C) is a transient configuration along the carbamoylation pathway, significantly less stable than the reactants (A). It lies 18.0 kcal mol^{-1} above the reactants for the p-hydroxy analogue, compared to 16.8 kcal mol^{-1} for the p-amino variant, and 15.8 kcal mol^{-1} for URB524. Expulsion of the biphenate leaving group gives carbamoylated Ser241 (E) overcoming small energy barriers (lower than 2 kcal mol^{-1}), suggesting that

Table 1 Interatomic distances (Å) for reactant (A) and TS (B) structures[a]

Structure	N_1–H_2	O_2–H_2	O_2–H_1	O_1–H_1	O_1–C
$URB524_A$	1.77	0.97	1.81	0.96	2.65
$URB694_A$	1.77	0.97	1.80	0.96	2.66
$URB618_A$	1.77	0.97	1.80	0.96	2.66
$URB524_B$	1.06	1.66	1.09	1.33	1.78
$URB694_B$	1.04	1.65	1.33	1.13	1.74
$URB618_B$	1.05	1.66	1.26	1.09	1.83

[a] Atom labels consistent with Fig. 2 and 4.

formation and collapse of TI are highly concerted. Calculations also show that, in contrast to FAAH substrates (e.g. oleamide and oleoylmethylester),[22] the expulsion of the leaving group occurs e ectively without prior protonation. However, protonation of the leaving group is required to conclude the catalytic cycle. It is facilitated by Ser217, which is well oriented both to deprotonate the positively charged Lys142 and to protonate the oxygen of the biphenate anion. Energy barriers for this step are small, $\sim$3 kcal mol^{-1} for URB524, $\sim$2 kcal mol^{-1} for URB694 and $\sim$3 kcal mol^{-1} for URB618, with respect to E. The final product (G) is the most stable configuration of the pathway. All the covalently inhibited complexes are relatively very stable (17 kcal mol^{-1} lower in energy than A for URB524, and by 13 and 11 kcal mol^{-1} for URB618 and URB694, respectively).

The QM/MM results presented here provide a mechanistic explanation for the observed lack of correlation between inhibitory potency and reactivity of these carbamates. The rate-limiting step for FAAH carbamoylation is the activation of Ser241, with the TS structure dominated by the proton transfer between Ser241 and Ser217. Conversely, for reactions with ''o -target'' carboxylesterases, reactivity of O-biphenyl-3-yl carbamates correlates well with inhibitor potency.[13]

DTSS calculations (details in ESIw) indicate that TS structures for Ser241 carbamoylation are greatly stabilized, compared to Michaelis complexes, for all three inhibitors. This stabilization is mainly related to residues involved in the proton transfer from Ser241 to Lys142, through Ser217. FAAH active site (Fig. 5 and Table S1, ESIw), provides comparable DTSS for all inhibitors (–25.1, −24.0, and −25.4 kcal mol^{-1} for URB524, URB694, and URB618, respectively). The highest contribution to the lowering of activation barriers is from Thr236 ($\sim$−7.5 kcal mol^{-1}). This residue accepts a H-bond from Lys142, and favours its protonation,[23] critical for Ser241 activation.[3] Ser218 (which also accepts a H-bond from Lys142), Ile238, Gly239 and Gly240 contribute comparable amounts of DTSS for the three inhibitors. Other amino acids show negligible contributions, with the exception of Asp237, which shows a small destabilizing e ect on the TS of URB618. The water molecule (Wat627, Fig. 3), involved in the recognition of p-OH and p-NH_2 substituents,[7] has a negligible contribution to TS stabilization (DTSS of −0.4 and −0.7 kcal mol^{-1} for URB694 and URB618, respectively).

The calculations reported here show that the mechanism of FAAH inhibition by URB524 and its derivatives gives similar barrier heights for carbamates that have significantly di erent reactivity. As intrinsic reactivity of carbamate-based inhibitors strongly a ects their pharmacokinetics and selectivity, QM/MM calculations may be useful for the design of new inhibitors with improved pharmaceutical properties

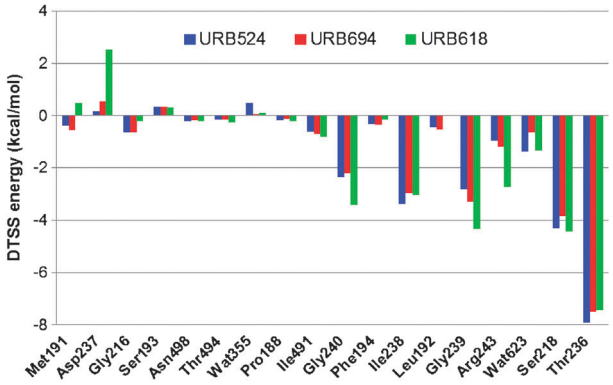

Fig. 5 DTSS energies at the MP2/6-31G(d) level of theory, for the carbamoylation of Ser241 with the three carbamate inhibitors.

e.g. improved in vivo potency and better selectivity vs. putative o -targets.

AJM and EC thank EPSRC for support. JS thanks the Royal Thai Government for funding.

Notes and references

1 M. Seierstad and J. G. Breitenbucher, J. Med. Chem., 2008, 51, 7327.
2 M. K. McKinney and B. F. Cravatt, Annu. Rev. Biochem., 2005, 74, 411.
3 A. Lodola, M. Mor, J. C. Hermann, G. Tarzia, D. Piomelli and A. J. Mulholland, Chem. Commun., 2005, 4399.
4 I. Tubert-Brohman, O. Acevedo and W. L. Jorgensen, J. Am. Chem. Soc., 2006, 128, 16904.
5 D. Piomelli, G. Tarzia, A. Duranti, A. Tontini, M. Mor, T. R. Compton, O. Dasse, E. P. Monaghan, J. A. Parrott and D. Putman, CNS Drug Rev., 2006, 12, 21.
6 E. Basso, A. Duranti, M. Mor, D. Piomelli, A. Tontini, G. Tarzia and P. Traldi, J. Mass Spectrom., 2004, 39, 1450.
7 G. Tarzia, A. Duranti, G. Gatti, G. Piersanti, A. Tontini, S. Rivara, A. Lodola, P. V. Plazzi, M. Mor, S. Kathuria and D. Piomelli, ChemMedChem, 2006, 1, 130.
8 M. J. Field, P. A Bash and M. Karplus, J. Comput. Chem., 1990, 11, 700.
9 A. Lodola, M. Mor, S. Rivara, C. Christov, G. Tarzia, D. Piomelli and A. J. Mulholland, Chem. Commun., 2008, 214.
10 J. P. Alexander and B. F. Cravatt, Chem. Biol., 2005, 12, 1179.
11 M. Mileni, S. Kamtekar, D. C. Wood, T. E. Benson, B. F. Cravatt and R. C. Stevens, J. Mol. Biol., 2010, 400, 753.
12 J. R. Clapper, F. Vacondio, A. R. King, A. Duranti, A. Tontini, C. Silva, S. Sanchini, G. Tarzia, M. Mor and D. Piomelli, ChemMedChem, 2009, 4, 1505.
13 F. Vacondio, C. Silva, A. Lodola, A. Fioni, S. Rivara, A. Duranti, A. Tontini, S. Sanchini, J. R. Clapper, D. Piomelli, M. Mor and G. Tarzia, ChemMedChem, 2009, 4, 1495.
14 W. A. Sokalski, J. Mol. Catal., 1985, 30, 395.
15 B. Szefczyk, A. J. Mulholland, K. E. Ranaghan and W. A. Sokalski, J. Am. Chem. Soc., 2004, 126, 16148.
16 M. Mor, A. Lodola, S. Rivara, F. Vacondio, A. Duranti, A. Tontini, S. Sanchini, G. Piersanti, J. R. Clapper, A. R. King, G. Tarzia and D. Piomelli, J. Med. Chem., 2008, 51, 7327.
17 Jaguar 6.0, Schrodinger, LLC, Portland, Oregon, 2005.
18 H. M. Senn and W. Thiel, Angew. Chem., Int. Ed., 2009, 48, 1198.
19 M. W. van der Kamp and A. J. Mulholland, Nat. Prod. Rep., 2008, 25, 1001.
20 M. Mileni, J. Garfunkle, C. Ezzili, F. S. Kimball, B. F. Cravatt, R. C. Stevens and D. L. Boger, J. Med. Chem., 2010, 53, 230.
21 H. Van de Waterbeemd, N. El Tayar, P. A. Carrupt and B. Testa, J. Comput.-Aided Mol. Des., 1989, 3, 111.
22 A. Lodola, M. Mor, J. Sirirak and A. J. Mulholland, Biochem. Soc. Trans., 2009, 37, 363.
23 A. Lodola, J. Sirirak, N. Fey, S. Rivara, M. Mor and A. J. Mulholland, J. Chem. Theory Comput., 2010, 6, 2948.